

Discrete event simulation of large-scale spatial continuous systems

Alexandre Muzy, Antoine Aiello,
Paul-Antoine Santoni
University of Corsica
SPE – UMR CNRS 6134
B.P. 52, Campus Grossetti, 20250 Corti.
FRANCE.
Emails: {a.muzy, aiello, santoni}@univ-corse.fr

Bernard .P. Zeigler, James .J. Nutaro,
Rajanikanth Jammalamadaka
Arizona Center for Integrative Modeling and
Simulation
University of Arizona
Tucson, AZ, United-States of America
Emails: {zeigler, nutaro, rajani}@ece.arizona.edu

Abstract – Complex spatially-extended systems consist of numerous sub-systems leading to large simulation execution times. One approach to reducing these execution times is designing a simulation engine to allocate its attention to sub-systems in proportion to their activity levels. In this paper, we consider a large scale simulation of a physics-based fire spread model. This model is discretized using a recently developed numerical method called quantization and implemented using discrete event simulation. In this paper, we provide comparisons between the quantization method and usual Euler discrete-time methods. The aim is to demonstrate the ability of quantization and discrete event simulation to focus on active sub-systems, thus significantly reducing execution time for large heterogeneous systems.

Keywords: *DEVS, quantization, large-scale spatial continuous systems, fire spread simulation.*

1 Introduction

Modeling and simulation of large-scale spatial systems often necessitates a long process starting from analysis and ending with a solution design. Large-scale spatial systems are generally composed of many sub-systems. Hence, at every step of the modeling process, the different models developed have to be designed to support efficient simulation. Simulation efficiency is inversely related to simulation complexity. The latter can be categorized into the following three areas: (i) quantity of information to store, (ii) quantity of information to exchange, and (iii) number of computations performed. Reducing this

complexity will result in decreasing execution time of the simulation.

In order to illustrate an example of a large-scale spatial continuous system, we will consider that the modeling process starts with the definition of a partial differential equation (PDE). PDEs allow us to capture spatial and temporal continuity of the real world through a formal mathematical language. In order to be simulated on a digital computer, PDEs have to be discretized into spatially arrayed cells and discrete-time steps. To achieve these goals, it is common to use conventional discrete-time methods (Euler, Adams, etc.) [1]. Basically, to solve a PDE, these methods necessitate computation of every cell's state even though there may be no significant state changes at many of the cells. In this context, the usual discrete-time numerical methods can result in more complex simulations than necessary.

To reduce the simulation complexity, one can define an algorithm that reduces the calculation domain by scanning cells' states [2]. However, this solution consists in artificially reducing the calculation domain independently of the numerical method.

Recently, a new numerical method based on discrete events has been proposed: cell state quantization [3, 4]. Values of state variables are discretized in equal quanta. Threshold crossings of a quantum lead to discrete event state transitions and inter-cell state updates. Time advances needed for the state to change a quantum amount are computed only for active cells, i.e., cells that have changed states by this amount. This original

method allows a discrete event simulator to faithfully track activity in space and thereby reduce execution times. There is a well-defined process for discretization of a PDE (or its quantization) to its implementation in Discrete Event System Specification (DEVS) [3].

In this paper we experiment with the quantization method on the complex phenomenon of fire spread. Indeed, this phenomenon is complex at every modeling step. First, complexity of the phenomenon is related to the high number of intricate physical phenomena composing fire spread. Second, precise physical models of fire spread, based on PDEs, have non-linear terms and therefore are not amenable to analytical solutions. Finally, to reduce execution times, spatial simulation has to focus on cells changing temperature rapidly around the fire front.

We will rigorously compare quantization of a physical model of fire spread to a reference Euler method. Both explicit and implicit methods will be explored. Explicit methods or Forward Euler methods compute the value of every cell of the cellular model at the next time step based on the values of these cells at the current time step. Implicit methods or Backward Euler methods use more sophisticated error convergence criteria to do the same calculation. Execution times of the different approaches will be compared. Since the physical model of fire spread has no analytical solution, the quantization results were compared to experimentally validated explicit results using an average relative error calculation. All the numerical methods' results were visually validated using laboratory experiments comparing simulated and experimental fire fronts positions.

2 Background

Quantization concepts are strongly related to discrete events. DEVS is thus a naturally appropriate framework to specify quantization models.

2.1 Quantization concepts

Quantization of ODEs has been introduced in [3, 5, 6]. Instead of generating approximate solutions at discrete points in time, the solution is approximated by looking at significant changes in the system's state. The magnitude of change in the

solution that is considered to be significant is called an integration quantum (or quantum). A quantum can be defined by:

$$D = |\Phi^{n+1} - \Phi^n| \quad (1)$$

Where D is the desired change in the solution at each step of the computation, Φ^{n+1} and Φ^n are two numerical approximations of the continuous function $\Phi(t)$ representing a time invariant process.

Using the explicit Euler formulae leads to:

$$\Phi^{n+1} = \Phi^n + \Delta t \cdot f(\Phi^n) \quad (2)$$

The time required for a quantum change to occur can be approximated by:

$$\Delta t = \frac{D}{|f(\Phi^n)|} \quad (3)$$

If $f(\Phi^n) = 0$, then $\Delta t \rightarrow \infty$, which indicates that an equilibrium is reached. Hence, no information is lost by setting $\Delta t \rightarrow \infty$.

A quantized integration scheme can be constructed by substituting equation (3) into equation (2) and keeping track of the sign of the derivative to ensure that the solution moves in the proper direction. This gives the system:

$$\Phi^{n+1} = \Phi^n + D \cdot \text{sign}(f(\Phi^n)) \quad (4)$$

Which approximates successive values of the continuous system. The time $t_{n+1} \in \mathfrak{R}$ of approximated states is given by:

$$t_{n+1} = t_n + \frac{D}{|f(\Phi^n)|} \quad (5)$$

An approximation example of the function $\Phi(t)$ is sketched in Figure 1. One can notice that for a continuous time base, the number of computations needed to approximate the curve $\Phi(t)$ can be reduced, even more when the latter changes slowly during time.

Equations (4) and (5) constitute a quantized integrator. In space, and when applied to PDEs, using such integrators allows to track activity, that is, changes in time in one point of the space. Then,

each integrator can be implemented as an atomic model DEVS.

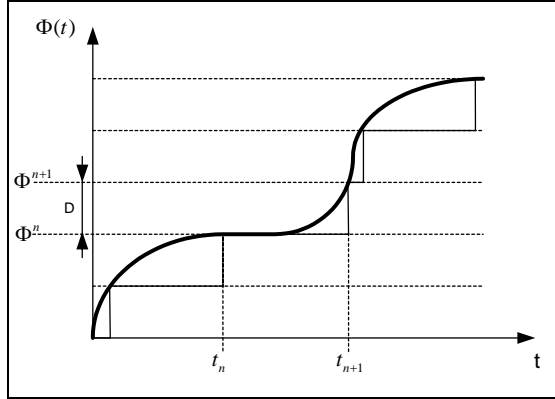


Figure 1. Quantization approximation of ODE

2.2 The DEVS formalism

Specification of cellular models can be achieved using the DEVS formalism. A DEVS Atomic Model (AM) is a structure [3]:

$$AM = \langle X, Y, S, \delta_{ext}, \delta_{int}, \delta_{conf}, \lambda, t_a \rangle$$

Where, X is the set of input values, Y is the set of output values, S is the set of sequential states, $\delta_{ext} : Q \times X^b \rightarrow S$ is the external transition function (where $Q = \{(s, e) / s \in S, 0 \leq e \leq t_a(s)\}$ is the total set of states, e is the elapsed time since the last state change, and $X^b \in X$ is a bag of input values), $\delta_{int} : S \rightarrow S$ is the internal transition function, $\delta_{conf} : S \times X^b \rightarrow S$ is the confluent transition function, $\lambda : S \rightarrow Y^b$ is the output function, $Y^b \in Y$ is a bag of output values, and $t_a : S \rightarrow \mathfrak{R}^+$ is the time advance function.

An atomic model allows specifying the behavior of a system. Connections between different atomic models can be performed by a coupled model (CM) [3]:

$$CM = \langle X, Y, D, \{M_i\}, \{I_i\}, \{Z_{i,j}\} \rangle$$

Where, X is the set of input values, Y is the set of output values, D is the set of model

references, For each $i \in D$, M_i is an atomic model, I_i is the influencer set, $Z_{i,j}$ is a function: the i to j output translation with (c.f. Figure 1): $Z_{MC,j} : X_{MC} \rightarrow X_j$ is the input coupling function, $Z_{i,MC} : Y_i \rightarrow Y_{MC}$ is the output coupling function, and $Z_{i,j} : Y_i \rightarrow X_j$ is the internal coupling function.

3 Fire spread modeling

To be simulated, physical fire spread models usually consist of reaction diffusion equations [7]. These PDEs cannot be solved analytically. They have to be solved numerically. Discrete-time solutions can be obtained using Explicit (Forward) or Implicit (Backward) Euler methods.

3.1 Physical model

The physical model we use [8] is composed of elementary cells of earth and plant matter. Under no wind and no slope conditions, the temperature of every cell is represented by the following PDE:

$$\frac{\partial T}{\partial t} = -k(T - T_a) + K \left(\frac{\partial^2 T}{\partial x^2} + \frac{\partial^2 T}{\partial y^2} \right) - Q \frac{\partial \sigma_v}{\partial t} \quad (6a)$$

$$\sigma_v = \sigma_{v0} \text{ if } T < T_{ig} \quad (6b)$$

$$\sigma_v = \sigma_{v0} e^{-\alpha(t-t_{ig})} \text{ if } T \geq T_{ig} \quad (6c)$$

$$T(x, y, t) = T_a \text{ at the boundary} \quad (6d)$$

$$T(x, y, t) \geq T_{ig} \text{ for the burning cells} \quad (6e)$$

$$T(x, y, 0) = T_a \text{ for the non burning cells at } t=0 \quad (6f)$$

Where, T_a (27 °C) is the ambient temperature, T_{ig} (300 °C) is the ignition temperature, t_{ig} (s) is the ignition time, T (°C) is the temperature, K ($m^2 \cdot s^{-1}$) is the thermal diffusivity, Q ($m^2 \cdot ^\circ C / kg$) is the reduced combustion enthalpy, α (s^{-1}) combustion time constant, σ_v ($kg \cdot m^{-2}$) is the vegetable surface mass, σ_{v0} ($kg \cdot m^{-2}$) is the initial vegetable surface mass (before the cell's combustion).

The term $k(T - T_a)$ represents thermal exchanges

with the air, the term $K \left(\frac{\partial^2 T}{\partial x^2} + \frac{\partial^2 T}{\partial y^2} \right)$ represents the

diffusion phenomenon and the term $Q \frac{\partial \sigma_v}{\partial a}$ represents the combustion energy (the reaction).

3.2 Discrete-time solutions

In a previous study, Finite Element and the Finite Difference Methods have been used to discretize the previous physical model [9]. The Finite Difference Method provided equivalent results as the Finite Element Method. However, the latter appeared more complex to implement and involved longer execution times. Therefore, the Finite Difference Method has been chosen.

3.2.1 The explicit solution

The physical model (6.a-f) solved by the Explicit Method leads to the following algebraic equation:

$$T_{i,j}^{n+1} = a(T_{i-1,j}^n + T_{i+1,j}^n) + b(T_{i,j-1}^n + T_{i,j+1}^n) + cQ \left(\frac{\partial \sigma_v}{\partial a} \right)_{i,j}^n + dT_{i,j}^n + e \quad (7)$$

Where, T_{ij} is the grid node temperature. The coefficients a , b , c , d and e depend on the time step and the mesh size considered.

The study domain is meshed uniformly with cells of 1-cm^2 and a time step of 0.01s . The propagation domain thus consists of a cellular model where each future cell's temperature is calculated using the current cell's temperature and temperatures of the cardinal neighbors.

3.2.2 The implicit solution

Implicit methods are typically more stable than explicit methods and allow larger time steps thus reducing execution times.

The physical model (6.a-f) solved by the Implicit Method leads to the following algebraic equation:

$$T_{i,j}^{n+1} = a'(T_{i-1,j}^{n+1} + T_{i+1,j}^{n+1}) + b'(T_{i,j-1}^{n+1} + T_{i,j+1}^{n+1}) + c'Q \left(\frac{\partial \sigma_v}{\partial a} \right)_{i,j}^{n+1} + d'T_{i,j}^{n+1} + e' \quad (8.a)$$

$$|T_{i,j}^{k+1,n+1} - T_{i,j}^{k,n+1}| < \varepsilon \quad (8.b)$$

Where, k is the iteration step. The coefficients a' , b' , c' , d' and e' depend on the time step and on the mesh size considered.

The solution is calculated at each time step using the iterative method of Jacobi [10] for which the convergence condition (8.b) is used to pass on to

the next time step. Hence, as long as all the whole temperatures calculated between two successive iterations are not less than an ε (10^{-3}K for example), the simulation clock is not incremented.

3.3 The Quantization solution

Quantization of equation (6a) consists of discretizing the term of thermal exchanges, the diffusion term and the reaction term. Then, in every cell a quantized integrator (*c.f.* equations (4) and (5)) calculates the temperature of the cell according to the value of: (1) the term of thermal exchanges (which is discretized), (2) the term of diffusion (which is discretized), and (3) the reaction term (which is quantized).

The discretization of the diffusion term in space using the center differences leads to:

$$K \left(\frac{\partial^2 T}{\partial x^2} + \frac{\partial^2 T}{\partial y^2} \right) \approx K \left(\frac{T_{i,j-1}^n - 2T_{i,j}^n + T_{i,j+1}^n}{(\Delta x)^2} + \frac{T_{i,j-1}^n - 2T_{i,j}^n + T_{i,j+1}^n}{(\Delta y)^2} \right) \quad (9)$$

The term of thermal exchanges can be directly discretized:

$$k(T - T_a) = k(T_{i,j}^n - T_a) \quad (10)$$

When the cell is burning, the energy $Q \frac{\partial \sigma_v}{\partial a}$ released by the combustion depends directly on the exponential decrease of the fuel mass:

$$\sigma_v = Q \sigma_{v0} e^{-\alpha(t-t_{ig})}, \text{ if } T \geq T_{ig} \quad (11)$$

By knowing that the fuel mass will decrease only by one quantum D , we obtain:

$$\sigma_v - D = Q \sigma_{v0} e^{-\alpha t} \quad (12)$$

Taking the logarithm, we obtain the time advance t_a :

$$ta = \frac{1}{\alpha} \ln \frac{\sigma_v - D}{Q \sigma_{v0}} \quad (13)$$

In every cell, the global time advance depends on this time advance (13). Every cell is a coupled model composed of two atomic models. Figure 2 describes this coupled model (CM). The latter is composed of an atomic model of Fuel Decrease

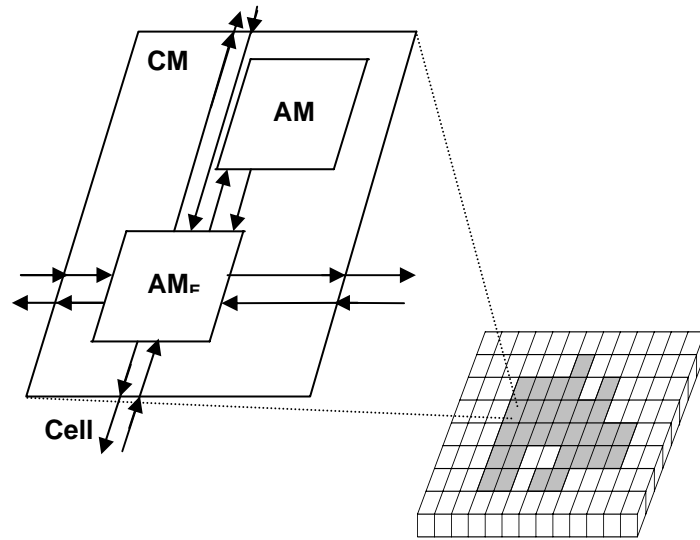


Figure 2. Cell description

(AM_{FD}) and of an atomic model of Thermal Exchanges and Diffusion (AM_{ED}).

An atomic model AM_{ED} is connected to its four cardinal neighbors through eight ports. Cells' temperatures are sent and received through these ports.

An atomic model AM_{FD} describes the evolution of the fuel mass decrease when the cell is burning. After the reception of the cell's temperature (contained in AM_{ED}), if the cell is in combustion, the external transition function of AM_{FD} will compute the time of next quantum boundary crossing according to the time advance (13). At each quantum crossing, computed by an internal transition, influenced cells are updated immediately. Finally, the derivative of the temperature, calculated by AM_{ED} , according to the neighboring cells' temperatures and to the fuel mass, is integrated using equations (4) and (5).

4 Simulation results

To validate the simulation results, experimental fires have been conducted on *Pinus Pinaster* litter, in a closed room without any air motion, at the INRA (Institut National de la Recherche Agronomique) laboratory near Avignon, France [8]. These experiments have been performed in order to observe fire spread for point-ignition fires under no slope and no wind conditions. The experimental apparatus was composed of a one

square meter aluminum plate protected by sand. A porous fuel bed was used, made up of pure oven dried pine needles spread as evenly as possible on the total area of the combustion table (in order to obtain a homogeneous structure). The experiment consisted in igniting a point using alcohol. The resulting spread of the flame across the needles has been closely observed with a camera and thermocouples.

The fuel mass decrease simulated by the atomic model AM_{FD} is represented in Figure 3. The end of this negative exponential curve pinpoints the interest of using a discrete event simulation passing directly from one continuous value of time to another. This allows to reduce the number of state transitions. However, the quantum size of this atomic model has to be carefully chosen because of the important beginning decreasing slope of the exponential curve. A too big quantum size leads to important errors. A quantum of $0.01\text{kg}/\text{m}^2$ has been chosen for this model.

As equation (6a) does not have analytical solution, the quantization simulation results are visually validated through the laboratory experiment. Moreover, an average relative error is calculated against the explicit simulation results already validated through numerous studies [8]:

$$\varepsilon = \sum_{i=1}^N \frac{1 - \frac{q_i}{q_i^*}}{N}$$

With N = number of cells,
 q_i = explicit value of cell i ,
 q_i^* = numerical value of cell i .

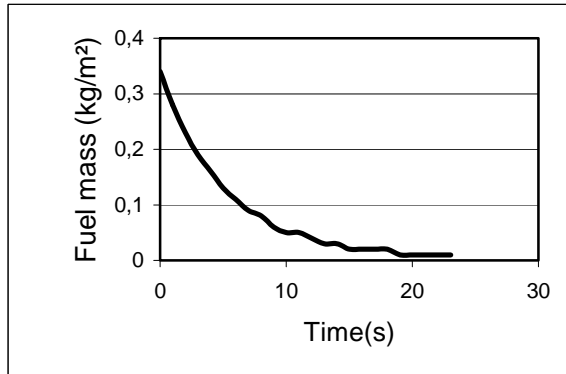


Figure 3. Fuel mass decrease using a continuous time base

Figure 6 depicts a visual comparison between the simulated fire fronts (using the explicit, implicit and quantization methods) and experimental fire fronts (white boxes). Explicit, implicit and quantization solutions are the same.

Figure 4 depicts the focus of the quantization simulation on active cells. The fire fronts are represented by lines. We can notice that the quantization simulation follows the fire front evolutions.

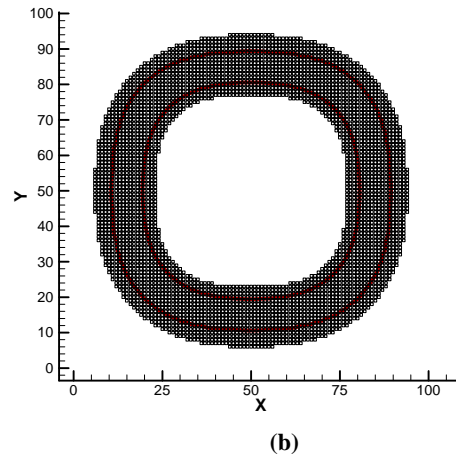
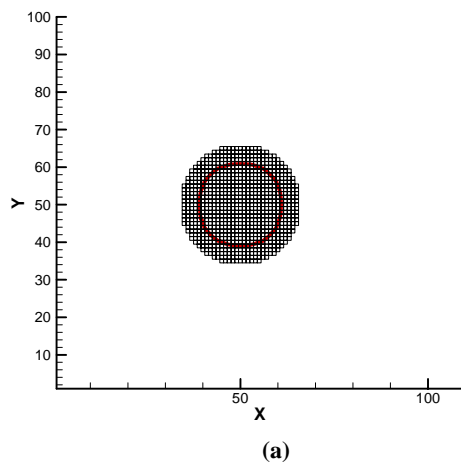


Figure 4. Focus of the quantization simulation on active cells at (a) 75s and (b) 122s

Figure 5 depicts the average relative error for different quantum sizes of the AM_{ED} atomic model, and the same experiment. This curve is almost linear. For very small quantum values, the error is constant. This means that the quantization solution is very close to the actual propagation.

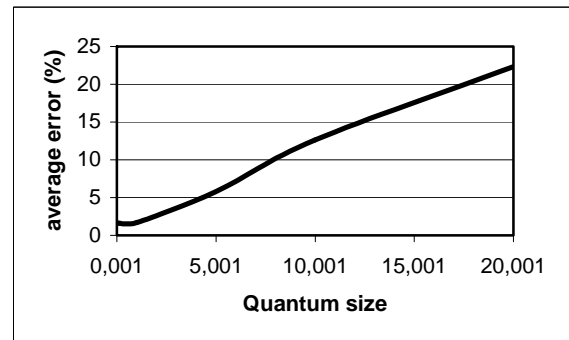


Figure 5. Average relative error for different quantum sizes

Figure 7 depicts the execution times and the number of transitions of the quantization solution, according to different quantum sizes. The more the quantum size is, the less the execution times and the number of transitions are. Moreover, until a quantum size of $5K$, both execution times and number of transitions decrease rapidly.

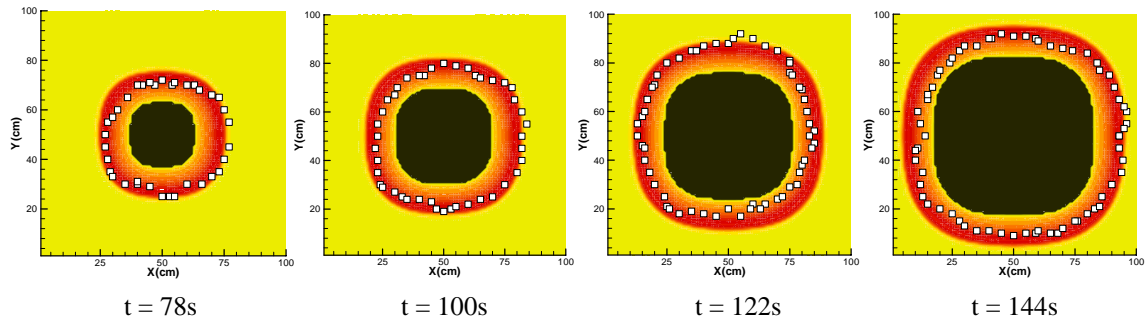


Figure 6. Visual comparison of simulated and experimental fire fronts

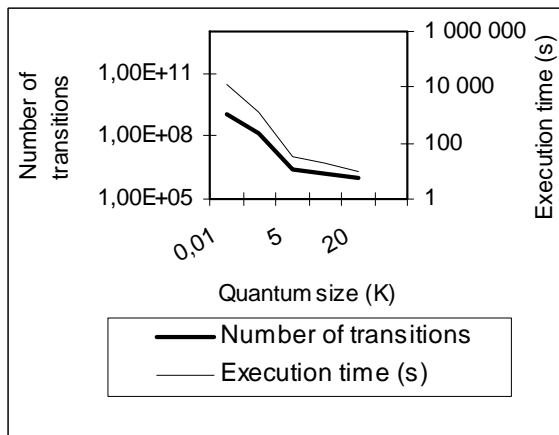


Figure 7. Execution times and number of transitions for different quantum sizes

Figure 8 depicts the execution times of the explicit, implicit and quantization solutions, for different propagation domain sizes, that is for different numbers of cells. For the quantization solution, a quantum size of $5K$ has been chosen thus leading to an approximate error of 5% . Concerning the implicit solution, using a bigger time step allows to reduce execution times. However, quantization execution times are significantly smaller. These good results can be explained by looking at Figure 9, which depicts the number of transitions of the different methods, for different propagation domain sizes. Indeed, the quantization method greatly reduces the number of transitions.

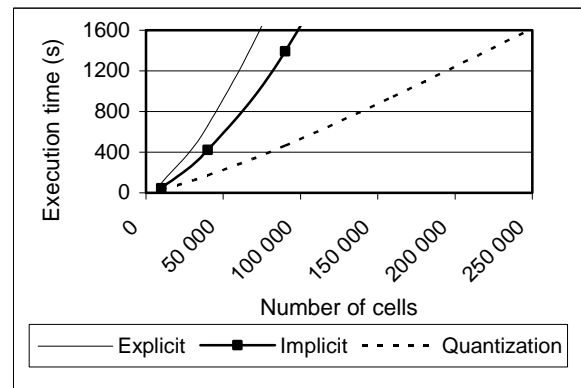


Figure 8. Execution times of the numerical solutions for different domain sizes

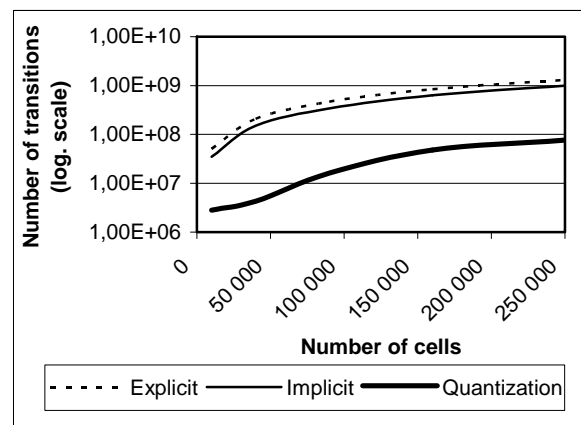


Figure 9. Number of transitions for different domain sizes

5 Conclusion

Quantization has been applied here to a complex system. It has been proved that it reduces execution times by naturally focusing computations on active cells of a large-scale cellular model.

However, to assess its benefits more generally, quantization has to be applied to other kinds of PDEs. Moreover, there are other methods that may offer advantages such as the conventional discrete-time methods coupled with an algorithm scanning active cells through Dynamic Structure Cellular Automata (DSCA) [11]. Comparisons between quantization, with its ability to focus on high activity regions and such modified methods will provide a better understanding of the advantages of each approach.

References

- [1] Ralston A, Rabinowitz P. 2001. *A First Course in Numerical Analysis*: Dover Publications.
- [2] Muzy A, Innocenti E, Hill D, Santucci JF. 2003. *Optimization of cell spaces simulation for the modelling of fire spreading*. Presented at 36th Annual Simulation Symposium, Orlando, USA. 289-96.
- [3] Zeigler BP, Praehofer H, Kim TG. 2000. *Theory of modelling and simulation*: Academic Press.
- [4] Kofman E. 2003. *Discrete event based simulation and control of continuous systems*. Ph.D. Dissertation thesis. Faculty of Exact Sciences, National University of Rosario, Argentina, Rosario.
- [5] Nutaro J. 2003. *Parallel discrete event simulation with applications to continuous systems*. Computer science PhD thesis. University of Arizona, Tucson.
- [6] Bolduc JS, Vangheluwe H. 2002. *Expressing ODE models as DEVS: Quantization approaches*. Presented at AI, Simulation and Planning in High Autonomy Systems, SCS, Lisboa, Portugal. 163-9.
- [7] Weber RO. 1991. *Toward a comprehensive wildfire spread model*. *International Journal of Wildland Fire* 1: 245-8.
- [8] Balbi JH, Santoni PA, Dupuy JL. 1998. *Dynamic modelling of fire spread across a fuel bed*. *Int. J. Wildland Fire* 9: 275-84.
- [9] Santoni PA. 1996. *Forest fire propagation: Dynamic modeling and numerical resolution, validation on fuel bed fires [in French]*. Ph.D. Thesis thesis. Università di Corsica, Corti.
- [10] Sibony M, Mardon JC. 1988. *Approximations et équations différentielles*: Hermann.
- [11] Muzy A, Innocenti E, Hill DRC, Aiello A, Santucci JF, Santoni PA. 2004. *Dynamic structure cellular automata in a fire spreading application*. Presented at First International Conference on Informatics in Control, Automation and Robotics, Setubal, Portugal. 143-51.